sp^3 and sp bonding characters.

The 27-GPa Raman spectrum is characteristic of graphite which is relatively well ordered, especially for shock-synthesized material. The crystal planar domain size, L_a, is estimated to be about 100 Å, based on the relative intensities of the 1355, 1580, and 2710 cm^{-1} bands (*19*). This dimension corresponds to a graphitic sheet of 5 to 10 planar-reconstructed C_{60} molecules. The peak mean bulk temperature 600°C is substantially lower than typical graphite annealing temperatures of 2000° to 3000°C (*20*). Thus, the graphite is formed primarily by high pressure. However, strong heterogeneous shock-heating near pores may assist the graphite formation. The temperatures during or after the unloading processes are too low for forming ordered graphite. Increasing disorder in the graphite products, as pressure and temperature increase, is in marked contrast to conventional thermal annealing effects on graphite (*20*).

The synthesis of graphite near 17 GPa is consistent with the static pressure results. The C_{60} ball is extremely incompressible and its molecular structure essentially remains unchanged at moderately high pressures. However, the center to center distance between nearest neighbor C_{60} molecules collapses from 10.0 Å at ambient pressure to 7.82 Å at 17 GPa (*3*), which is comparable to the C_{60} diameter 7.1 Å (*1*). Interfullerene C–C distances at 17 GPa are, then, expected to be close to the C=C bond length in C_{60} and in graphite (*21*). Under these circumstances graphite can be formed through π-electron rehybridization (a fast process) without involving a great deal of atomic rearrangement (a slow diffusive process). That is, when the distance between C atoms on adjacent fullerenes approaches the C–C separation within a fullerene, bonding arrangements probably change from intrafullerene to interfullerene in such a way as to collapse balls into planar graphite. Fast reorientation of electronic bonds is, thus, expected to enable this reconstructive phase transformation on a submicrosecond time scale.

As shown in Fig. 1, the *P-T* paths of C_{60} shocked below 30 GPa remain in a region where the graphite phase is metastable. At higher shock pressures the sample is driven above the graphite-diamond kinetic line, where graphite transforms directly to diamond on a fast (microsecond) time scale (*22*). However, recovery of diamond depends strongly on thermal path, nucleation and growth kinetics, and thermal quench rates (*22*). Thus, diamond probably formed during compression in the 100-GPa range at temperatures above 3000 K, but reverted to amorphous carbon during pressure release because of an insufficient thermal quench rate.

REFERENCES AND NOTES

1. H. W. Kroto, J. R. Heath, S. C. O'Brien, R. F. Curl, R. E. Smalley, *Nature* **318**, 162 (1985); W. Krätschmer, L. D. Lamb, K. Fostiropoulos, D. R. Huffmann, *ibid.* **347**, 354 (1990).
2. H. Kroto, *Science* **242**, 1139 (1988); T. G. Schnalz, W. A. Seitz, D. J. Klein, G. E. Hite, *J. Am. Chem. Soc.* **110**, 1113 (1988).
3. S. J. Duclos, K. Brister, R. C. Haddon, A. R. Kortan, F. A. Thiel, *Nature* **351**, 380 (1991).
4. Q.-Z. Zhang, J.-Y. Yi, J. Bernholc, *Phys. Rev. Lett.* **66**, 2633 (1991).
5. K.-A. Wang *et al.*, *Phys. Rev. B*, in press.
6. E. Edelson, *Popular Science* **239**, 52 (August 1991); A. F. Hebard *et al.*, *Nature* **350**, 600 (1991); M. S. Dresselhaus and G. Dresselhaus, a private communication.
7. R. M. Fleming *et al.*, *Bull. Am. Phys. Soc.* **36**, 352 (1991).
8. H. Hirai and K. I. Kondo, *Science* **253**, 772 (1991).
9. W. Utsumi and T. Yagi, *ibid.* **252**, 1542 (1991).
10. C. Maihiot and A. K. McMahan, in preparation.
11. D. J. Erskine and W. J. Nellis, *Nature* **349**, 317 (1991); P. S. DeCarli and J. C. Jamieson, *Science* **133**, 1821 (1961).
12. The C_{60} powder was obtained from Research Co. (Golden, CO). It contains approximately 85% of C_{60} and 15% of C_{70} based on mass spectrographic analysis. The presence of 15% of C_{70} is expected to have a weak effect on the results because of the disordered fluid-like nature of powder specimens.
13. For the experiments at 70 and 110 GPa the C_{60} powder is sandwiched between millimeter-thick Cu plates. This sample assembly is then loaded in a stainless steel recovery capsule and a maraging steel fixture.
14. J. J. Neumeier *et al.*, *High Pressure Res.* **1**, 267 (1989).
15. A one-dimensional Lagrangian wave propagation program POT (Projectile On Target) is used in the calculation. This program was originally developed by G. E. Duvall.
16. W. H. Gust, *Phys. Rev.* **B22**, 4744 (1980).
17. M. van Thiel and F. H. Ree, *Int. J. Thermophys.* **10**, 227 (1989).
18. M. van Thiel, F. H. Ree, R. Grover, in *Shock Waves in Condensed Matter*, S. C. Schmidt and N. C. Holmes, Eds. (Elsevier, New York, 1988), pp. 81–84.
19. D. S. Knight and W. B. White, *J. Mat. Res.* **4**, 385 (1989); R. J. Nemanich and S. A. Solin, *Phys. Rev.* **B20**, 392 (1979); D. S. Bethune *et al.*, *Chem. Phys. Lett.* **179**, 181 (1991); also see K. A. Wang *et al.* (*5*).
20. Graphitization of carbon typically occurs by an annealing process at high temperatures of 2000° to 3000°C, and the better ordered graphite is formed at the higher annealing temperatures. The 27-GPa Raman spectrum in Fig. 2 is similar to that of graphite annealed at 2200°C or above, reported in the references: R. Vidano and D. B. Fischbach, *J. Am. Ceramic Soc.* **61**, 13 (1978); P. Lespade, A. Marchand, M. Couzi, F. Cruege, *Carbon* **22**, 375 (1984); Y. Hishiyama, M. Inagaki, S. Kimura, S. Yamada, *ibid.* **12**, 249 (1974).
21. The bond length changes in the sp^2 type bonds are typically less than a few percent at the pressure of 20 GPa. It may well be applied to a case of C_{60}. Assuming 2% reduction in the C=C bond length of C_{60}, the ball diameter is estimated to be 6.35 Å at 17 GPa. The interatomic C–C distances are then 1.51 Å, which is similar to the C=C bond lengths in C_{60} (two bond lengths in the C_{60} cluster are 1.46 Å and 1.40 Å) and in graphite (the C=C length in the plane is 1.42 Å). Furthermore, it is expected that 2% reduction in the C=C bonds in C_{60} at 17 GPa may represent an upper limit.
22. F. P. Bundy, *J. Geophys. Res.* **85**, 6930 (1980); A. V. Kurdyumov, N. F. Ostrovskaya, A. N. Pilyankevich, *Sov. Powder Metal. Met. Ceram.* **27**, 32 (1988); A. M. Staver, N. V. Gubareva, A. I. Lyamkin, E. A. Petrov, *Sov. Combustion Explosion Shock Waves* **20**, 567 (1980); also see (*11*).

23. We are pleased to acknowledge the contributions of N. Hinsey and W. Brocious for technical assistance and gun operations. We thank H. Cynn at UCLA for numerous discussions about C_{60} and N. C. Holmes, M. van Thiel, and F. H. Ree at LLNL for discussions about thermal properties of carbon. This work was performed under the auspices of the U.S. Department of Energy by Lawrence Livermore National Laboratory under contract number W-7405-ENG-48.

17 September 1991; accepted 28 October 1991

Symbiont Recognition and Subsequent Morphogenesis as Early Events in an Animal-Bacterial Mutualism

MARGARET J. MCFALL-NGAI AND EDWARD G. RUBY

Bacterial colonization of the developing light organ of the squid *Euprymna scolopes* is shown to be highly specific, with the establishment of a successful association resulting only when the juvenile host is exposed to seawater containing one of a subset of *Vibrio fischeri* strains. Before a symbiotic infection the organ has elaborate epithelial structures covered with cilia and microvilli that are involved in the transfer of bacteria to the incipient symbiotic tissue. These structures regressed within days following infection; however, they were retained in uninfected animals, suggesting that the initiation of symbiosis influences, and is perhaps a prerequisite for, the normal developmental program of the juvenile host.

BENEFICIAL ASSOCIATIONS WITH SPECIFIC bacterial symbionts characterize many, if not all, animal species. Yet the mechanisms that determine recognition and specificity, or that control subsequent morphogenesis, in developing animal-bacterial mutualisms have remained remarkably undescribed. The light organ symbiosis between the squid *E. scolopes* and its monospecific culture of the luminous bacterium *V. fischeri* exhibits experimental advantages not found in other commonly studied animal-bacterial mutualisms. Specifically, the host

Department of Biological Sciences, University of Southern California, Los Angeles, California 90089–0371.

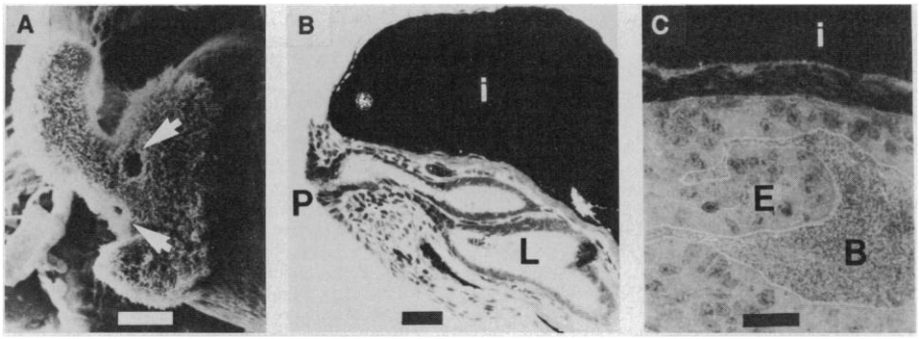

Fig. 1. Route of the infecting bacterial symbionts into light organ tissue. (**A**) Ventral view of one half of the juvenile light organ. Each of the two epithelial structures initially bears three pores, two of which (arrows) are visible in this scanning electron micrograph (*17*). Scale bar, 50 μm. (**B**) Cross section of the uninfected juvenile light organ. Each pore leads to one of three epithelial cell-lined lacunae on each side of the light organ. In the uninfected organ, these lacunae appear as empty sacs. Scale bar, 25 μm. (**C**) Cross section of the infected juvenile light organ. Within 24 hours of inoculation, symbiotic luminous bacteria have entered and begun to grow within the light organ, densely colonizing the lacunae (*16, 17*). Scale bar, 8 μm. B, bacteria; E, host epithelial cells; i, ink sac; L, lacuna; and P, pore.

has been successfully reared axenically under laboratory conditions (*1, 2*), and its luminous bacterial symbiont is a well-described and easily cultured species (*3*). These properties permit the experimentally controlled study of critical events in the establishment and maintenance of a symbiotic infection.

The mantle cavity of the adult *E. scolopes* contains a large, bilobed, light-emitting organ (*4*) in which is maintained about 10^7 cells of *V. fischeri*, a common species of luminous bacteria, related to such important animal-associated pathogens as *V. cholerae* and *V. parahaemolyticus* (*5*). The animal uses a number of differentiated tissue types (*4*) including a reflector, a muscle-derived lens, and a movable shutter, to modify the light emission during behavioral displays. This remarkably complex structure develops from a small rudiment in the center of the mantle cavity of a newly hatched squid. The rudiment is different from the adult organ in two important ways. First, it is free of symbiotic bacteria, which must be obtained anew by each juvenile host (*2*). Second, the rudiment bears a distinct structure on each of its lateral surfaces that facilitates the bacterial inoculation. Each structure consists of a large area of differentiated epithelial cells with a pair of anterior and posterior extensions that project into the mantle cavity. The entire structure is covered with a field of cilia and microvilli. Three pores occur at the base of each structure, and each pore (Fig. 1A) is an opening to a cilia-lined duct that leads into an interior, epithelium-lined space, or lacuna, within the incipient light organ (Fig. 1B).

Vibrio fischeri cells with the potential of infecting the lacunae are present in the seawater of the squid's habitat at an apparent concentration of less than 100 cells/ml (*6*). Thus, as this seawater is pumped through the mantle cavity during normal ventilation, the squid must facilitate the passage of at least one (or more) symbiosis-competent bacterium through the pores on the surface of the incipient light organ. This process is enhanced by the position of the organ, which occupies much of the volume of the funnel, the exit pathway for water leaving the mantle cavity. Further, the tips of the two ciliated, microvillous structures on each side of the organ come in close contact forming a hollow "ring" of tissue, with the entry pores located at the inside of the "ring." High-speed cinematography revealed that the effective beat of the cilia causes entrainment of the symbiont-containing water through this "ring" (*7*). This behavior can be expected to increase the probability that bacteria will approach and enter the pores and, if they are symbiosis-competent, produce the typical confined, benign infection that fills the lacunae (Fig. 1C).

Experimental manipulations of the infection process have shown it to be rapid and highly specific. Newly hatched squids failed to develop the capacity to emit bioluminescence when placed in filter-sterilized seawater (Fig. 2), even after an incubation of 10 days or more. However, placing juvenile squids in water to which had been added (per milliliter) 10^3 cells of certain strains of *V. fischeri* resulted in detectable light emission from the animal after 8 to 12 hours. The intensity of symbiotic luminescence in-

Table 1. Luminous bacterial strains capable of initiating a symbiosis in the juvenile *E. scolopes* light organ. Individual axenic squids (less than 24 hours post-hatch) were placed in vials containing 5 ml of filter-sterilized seawater to which the test bacterial strain (*15*) was added at a final density of about 10^3 cells per milliliter. After exposure to the inoculum for 12 hours at 25°C the squid was rinsed several times with, and subsequently maintained in, sterile seawater. A successful infection was judged by several criteria: the induction of symbiotic light emission by the squid (as shown in Fig. 2) and the presence of at least 10^5 cells of the inoculating strain in light organ homogenates (*16*). In addition, representative animals from each group were examined for histological evidence of bacterial colonization of the developing light organ (as shown in Fig. 1C).

Species	Animals infected
V. fischeri, symbiotic strains isolated from:	
E. scolopes (5)*	75 of 75
E. morsei (4)	17 of 17
M. japonicus (2)	22 of 22
V. fischeri, seawater strains isolated from:	
Kaneohe Bay, Hawaii (8)	33 of 33
Santa Monica Bay, California (6)	0 of 51
V. logei (3)	0 of 9
V. harveyi (3)	0 of 15
V. vulnificus (1)	0 of 3
P. leiognathi (4)	0 of 16
P. phosphoreum (3)	0 of 13

*Numbers in parentheses are the number of different strains tested.

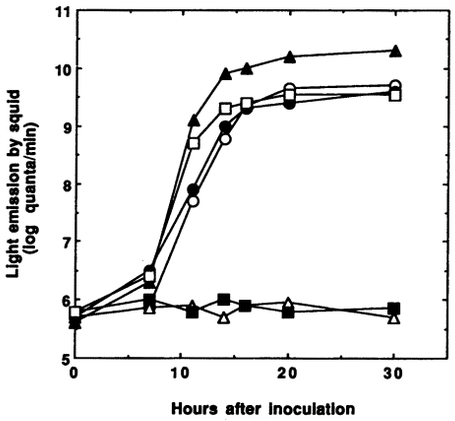

Fig. 2. Onset and development of symbiotic light emission by juvenile *E. scolopes* squids exposed to different seawater suspensions. Newly hatched, axenic animals were rinsed in filter-sterilized seawater, and placed in a small vial containing 5 ml of either sterile seawater (△) or sterile seawater to which was added (per milliliter) 10^3 cells of the following *V. fischeri* isolates (*15*): symbiotic strains obtained from the light organs of specimens of *E. scolopes* (●) and *E. morsei* (○), or a free-living strain isolated directly from Hawaiian seawater (▲). Other juvenile squid were, after rinsing, placed in vials containing coastal seawater either from Hawaii (□) or from Southern California (■). Each squid was exposed continuously to its test inoculum for 12 hours, then rinsed several times with, and resuspended in, sterile seawater. Bioluminescence of the animal was monitored periodically by placing its vial in a light-tight chamber containing a photomultiplier tube (PMT) (*3*). Background dark current of the PMT: 10^6 quanta per minute.

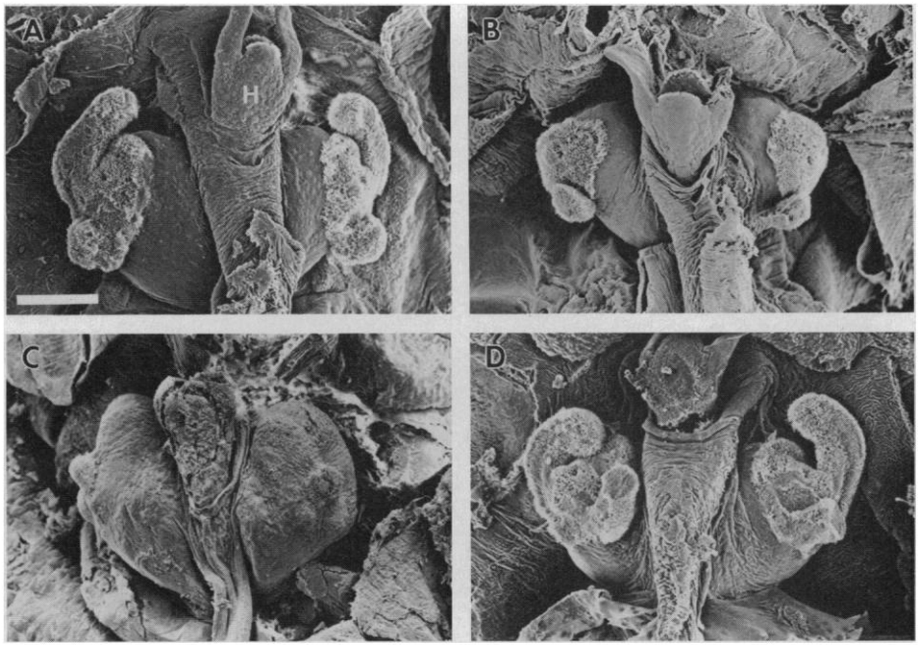

Fig. 3. Developmental program of the ciliated, microvillous epithelial tissue on the light organ of the juvenile squid. (**A**) At the time of hatching, the tissue occurs as elaborate bilateral structures on the surface of the incipient light organ. H, hindgut. (**B**) A 5-day-old juvenile squid that had been infected with symbionts immediately upon hatching. Much of the epithelial extensions are no longer apparent. (**C**) An 18-day-old symbiotic juvenile squid. (**D**) A 5-day-old uninoculated squid. All plates are at the same magnification; representative scale bar, 100 μm (*17*).

creased at an exponential rate, reaching approximately 10^4 times background levels within about 18 hours. This increase in light emission was paralleled by a rapid rise in bacterial numbers within the organ, approaching about 10^5 to 10^6 cells after 24 hours. Such rapid growth, combined with a thousand-fold induction in the specific activity of luciferase (*3*), the bacterial enzyme responsible for light emission, enabled the squid to produce within hours the visible levels of light emission characteristic of the symbiosis.

Most *V. fischeri* tested were competent symbionts (Fig. 2 and Table 1), including strains isolated from the light organs of adult *E. scolopes*, or the related squid, *E. morsei* (*8*), and two strains recently isolated from the light organs of specimens of the symbiotically bioluminescent fish, *Monocentris japonicus* (*9*). In addition, *V. fischeri* strains isolated directly from seawater collected from the habitat in which *E. scolopes* are found (Kaneohe Bay, Hawaii) were capable of initiating symbiosis. Interestingly, some strains of *V. fischeri*, such as those isolated from Santa Monica Bay, California, were unable to colonize the light organ (Table 1). These results suggest that important symbiotic determinants may not be present in all strains of *V. fischeri*.

The inability to initiate a symbiosis also extended to other species of luminous bacteria, including strains of *V. harveyi* and *Photobacterium leiognathi* that were isolated from seawater collected in the squid's natural habitat (*9*). Thus, even species of luminous bacteria that co-occur with, and are at least as abundant as (*6*), symbiosis-competent *V. fischeri* and that are found as symbionts in the light organs of other marine squids and fishes (*10*), cannot colonize *E. scolopes*.

Whereas a symbiotic association could be achieved by exposing hatchlings to nearshore seawater from their native Hawaiian habitat (Fig. 2), no successful infection resulted after exposure to seawater from coastal Southern California (Table 1). However, addition of symbiosis-competent bacteria to California seawater resulted in a typical infection process that was indistinguishable from that occurring with native Hawaiian seawater. Thus, the juvenile squid not only can select the appropriate species (and strain) of bacterium from the myriad of different bacteria present in natural seawater, but also can successfully resist nonspecific colonization when the ambient water does not contain the correct symbiotic strain. These results argue against a prevailing theory that the mechanism by which specificity is achieved in light organ symbioses is based primarily on the distinct physiological differences that exist between the species of luminous bacteria (*11*). Instead, these data provide the first evidence that a rapidly expressed mechanism, perhaps requiring the presence of symbiosis genes encoding a specific surface receptor or other signal factor (*12*), may be responsible for initiating species (and strain) specificity in light organ symbioses.

As in most animal-bacterial associations (*13*), the primary interaction in the *E. scolopes–V. fischeri* symbiosis occurs between the bacterium and the host's epithelium. Morphological data indicate that the initiation of this symbiosis is not only mediated by, but also affects the development of, the superficial, epithelial structures of the juvenile light organ (Fig. 3A). As early as the third day after inoculation of the light organ, the ciliated, microvillous surfaces that project into the mantle cavity were nearly absent (Fig. 3B). By 18 days the entire structure had completely disappeared (Fig. 3C), leaving only the single, lateral, ciliated pore that persists in the adult light organ condition (*4*). In contrast to this normal symbiotic pattern of development, the complete structure was retained by 5-day-old uninoculated juveniles that were maintained after hatching either in sterile seawater or in natural seawater containing symbiosis-incompetent strains of *V. fischeri* (Fig. 3D). Thus, the presence of symbiotic bacteria appears to signal further development and maturation of the light organ. In addition, such observations suggest that these structures are crucial specifically during the inoculation of the light organ, which would render them the only known example, in either animal or plant symbioses, of a tissue whose sole apparent function is to facilitate initiation of the association.

Animal developmental biology, while typically concerned with the essential processes of differential control of gene expression and signalling between developing cells of a single organism, must also be concerned with the fact that, in nature, organisms often develop normally only in the presence of associated microorganisms. For example, metabolic products and regulatory compounds encoded by the symbiont genome are required for normal post-embryonic development of the sexual organs in some insects and of epithelial tissue and the immune response in vertebrates (*14*). The squid–luminous bacteria symbiosis is an emerging experimental system that makes accessible the study of how such associations with microorganisms are integrated into the general developmental program of an animal.

REFERENCES AND NOTES

1. M. J. McFall-Ngai and E. G. Ruby, in *Endocytobiology*, P. Nardon, V. Gianinazzi-Pearson, A. M. Grenier, L. Margulis, D. C. Smith, Eds. (INRA, Paris, 1990), vol. 4, pp. 319–321; J. M. Arnold, C. T. Singley, L. D. Williams-Arnold, *Veliger* **14**, 361 (1972).

2. S. L. Wei and R. E. Young, *Mar. Biol.* **103**, 541 (1989).
3. K. J. Boettcher and E. G. Ruby, *J. Bacteriol.* **172**, 3701 (1990); E. A. Meighen, *Microbiol. Rev.* **55**, 123 (1991).
4. M. McFall-Ngai and M. K. Montgomery, *Biol. Bull.* **179**, 332 (1990).
5. P. A. Blake, R. E. Weaver, D. G. Hollis, *Annu. Rev. Microbiol.* **34**, 341 (1980); R. Sakazaki and A. Balows, in *The Prokaryotes*, M. P. Starr, H. Stolp, H. G. Truper, A. Balows, H. G. Schlegel, Eds. (Springer-Verlag, Berlin, 1981), vol. 2, chap. 103.
6. K.-H. Lee and E. G. Ruby, *Abstr. Annu. Meet. Am. Soc. Microbiol.* **91**, 194 (1991).
7. M. McFall-Ngai, unpublished data.
8. K. N. Nesis, *Cephalopods of the World* (T.F.H. Publications, Neptune City, NJ, 1982), p. 70.
9. Isolations of bacteria from animal light organs, or directly from seawater, were performed as described by K. H. Nealson [*Methods Enzymol.* **57**, 153 (1978)].
10. J. L. Reichelt, K. H. Nealson, J. W. Hastings, *Arch. Microbiol.* **112**, 157 (1977); S. Fukasawa and P. V. Dunlap, *Agric. Biol. Chem.* **50**, 1645 (1986).
11. J. W. Hastings, J. Makemson, P. V. Dunlap, *Symbiosis* **4**, 3 (1987).
12. S. R. Long, *Cell* **56**, 203 (1989); B. G. Rolfe and P. M. Gresshoff, *Annu. Rev. Plant Physiol. Plant Mol. Biol.* **39**, 297 (1988); L. J. Halvorson and G. Stacy, *Microbiol. Rev.* **50**, 193 (1986).
13. B. B. Finley and S. Falkow, *Microbiol. Rev.* **53**, 210 (1989); R. R. Isberg, *Science* **252**, 934 (1991).
14. K. J. Hackett, D. E. Lynn, D. L. Williamson, A. S. Ginsberg, R. F. Whitcomb, *Science* **232**, 1253 (1986); M. S. Gil-Turnes, M. E. Hay, W. Fenical, *ibid.* **246**, 116 (1989); H. A. Gordon and L. Pesti, *Bacteriol. Rev.* **35**, 390 (1971).
15. Strains of *V. fischeri* used in this study were isolated either from the light organs of sepiolid squids (four specimens of *E. scolopes* and three specimens of *E. morsei*) or a monocentrid fish (two specimens of *M. japonicus*), or directly from Hawaiian or Californian coastal seawater samples (*9*). The strains of *V. logei* and *V. vulnificus* were provided by R. Rossen. All strains of *V. harveyi* and two *P. leiognathi* and two *P. phosphoreum* strains were seawater isolates. The two other *P. leiognathi* strains and the third *P. phosphoreum* strain were isolated from the light organs of leiognathid and macrourid fishes, respectively. All of these bacterial species have growth rate optima between 25° and 30°C (*9*).
16. Twenty-four hours after exposure to a potential symbiotic bacterial inoculum, each juvenile *E. scolopes* was rinsed in sterile seawater, its incipient light organ was homogenized, and aliquots of the homogenate spread on a seawater-based agar medium to determine the extent of bacterial infection (*3*). Uninfected squids had an undetectable number of bacteria (<20) in homogenates of their light organs.
17. Juvenile squids were fixed for scanning electron microscopy in filtered seawater containing 2% paraformaldehyde and 2% glutaraldehyde, dehydrated in an ethanol series, critical-point dried, and sputter-coated with gold, before analysis on a Cambridge model 360 scanning electron microscope. For histology, animals were fixed for 24 hours in a 0.5 M sodium phosphate buffer (pH 7.5) containing 5% formaldehyde. Specimens were then dehydrated in an ethanol series, embedded in Spurr plastic resin, and sectioned at a thickness of 1.5 μm.
18. We thank M. Montgomery and R. Young for helpful discussions, R. Emlet for making possible high-speed cinematography of juvenile light organs, and J. McCosker, T. Okutani, and R. Young for help in obtaining animals for bacterial isolations. Histological sections were provided by M. Montgomery, and A. Thompson assisted with electron microscopy. Supported by NSF grant DMB-8917293 and ONR grant N00014-91-J-1357.

25 July 1991; accepted 17 October 1991

Selective Cleavage of Human DNA: RecA-Assisted Restriction Endonuclease (RARE) Cleavage

LANCE J. FERRIN AND R. DANIEL CAMERINI-OTERO*

Current methods for sequence-specific cleavage of large segments of DNA are severely limited because of the paucity of possible cleavage sites. A method is described whereby any Eco RI site can be targeted for specific cleavage. The technique is based on the ability of RecA protein from *Escherichia coli* to pair an oligonucleotide to its homologous sequence in duplex DNA and to form a three-stranded complex. This complex is protected from Eco RI methylase; after methylation and RecA protein removal, Eco RI restriction enzyme cleavage was limited to the site previously protected from methylation. When pairs of oligonucleotides are used, a specific fragment can be cleaved out of genomes. The method was tested on λ phage, *Escherichia coli*, and human DNA. Fragments exceeding 500 kilobases in length and yields exceeding 80 percent could be obtained.

MAPPING LARGE GENOMES WOULD be greatly simplified and accelerated by development of a facile method to perform sequence-specific cleavage of DNA. In previous attempts to perform sequence-specific cleavage of genomic DNA, essentially two independent strategies have been followed. The first strategy used the ability of synthetic homopyrimidine oligonucleotides to anneal to duplex homopyrimidine-homopurine tracts to form triple-helical structures and has been used by several investigators to cleave genomes as large as *Saccharomyces cerevisiae*. This approach was first used by Moser and Dervan (*1*) to cleave a plasmid by equipping the oligonucleotide with an EDTA-Fe cleavage moiety. Subsequently, other cleavage moieties were attached to homopyrimidine oligonucleotides (*2*), or guanine-rich oligonucleotides (*3*). The main disadvantage of this targeting approach is that only homopyrimidine or guanine-rich oligonucleotides have been used successfully. In a second strategy, Szybalski and co-workers cleaved *S. cerevisiae* and *E. coli* genomes at a single introduced *lac* operator site (*4*). They first methylated Hae II sites in the DNA by using the *lac* repressor to protect a Hae II site within the *lac* operator from methylation. After removal of the methylase and the repressor, the only Hae II site unmodified and available for cleavage was in the *lac* operator. The advantages of this approach were the high yield and the high specificity. The main disadvantage was that only a *lac* operator site could be cleaved, although the method has been extended to oligopyrimidine-binding sites (*5*).

In designing a general and efficient method to perform sequence-specific cleavage and targeting of genomic DNA, we have attempted to exploit the advantages of the first two strategies while avoiding the disadvantages. We have used the ability of recombinases to pair any oligonucleotide with its homologous duplex to form a three-stranded complex. This allows specific targeting of any desired sequence.

Recent work has established that recombinases such as the RecA protein can hybridize a single strand of any sequence to an intact duplex to form a novel DNA triplex in which the third strand may include both purines and pyrimidines (*6, 7*). For reasons that at this point are not clear, the protein-free structures that we have described can only be formed in good yields on the ends of duplexes (*6*). Recently, however, we have established that related (but not necessarily identical) structures coated with RecA protein can be formed and isolated in which the pairing need not be at an end of the duplex. In these structures a single strand as short as an oligonucleotide 15 bases long can be targeted to a homologous duplex (*8*). Furthermore, these complexes are resistant to

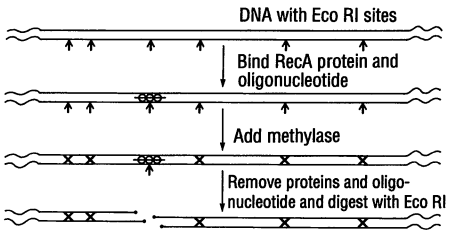

Fig. 1. Schematic of the strategy used for sequence-specific cleavage of DNA. An explanation is given in the text. This diagram shows cleavage at a single site, but a pair of oligonucleotides can be used to generate a DNA fragment. ↑, Eco RI site; **X**, methylated Eco RI site, and ⊖⊖⊖, RecA protein with an oligonucleotide.

Genetics and Biochemistry Branch, National Institute of Diabetes and Digestive and Kidney Diseases, National Institutes of Health, Bethesda, MD 20892.

*To whom correspondence should be addressed.